Measurement of radiation dose at the north interaction point of BEPCII*

Mo Xiaohu[1†], Zhang Jianyong[1], Zhang Tianbao[1], Zhang Qinjiang[1], Achasov Mikhail[3], Fu Chengdong[1,2], Muchnoi Nikolay[3], Qin Qing[1], Qu Huamin[1], Wang Yifang[1], Wu Jingming[1], Xu Jinqiang[1], Yu Boxiang[1]

1 (Institute of High Energy Physics, CAS, Beijing 100049, China)

2 (Tsinghua University, Beijing 100084, China)

3 (Budker Institute of Nuclear Physics, Novosibirsk 630090,Russia)

May 18, 2009

Abstract The technique details for measuring radiation dose are expounded. The results of radiation levels of gamma and neutron are presented and the corresponding radiation shielding is discussed based on the simplified estimation. In addition, the radiation level of photon as background for the future experiment is measured by NaI(Tl) detector.

Key words radiation dose, shielding thickness, photon background, NaI(Tl) detector

PACS 07.89.+b, 28.41.Qb, 29.40.Wk

1 Introduction

The large data sample to be collected at BESIII is typically a few fb^{-1} [1, 2], unprecedented statistical precision will be achieved in data analysis, hence many systematic factors and effects have to be considered seriously in order to obtain correct results with precision. As pointed out in Ref. [3] the uncertainty of the beam energy plays an important role for BESIII physics analyses in many aspects. First of all, the detailed Monte Carlo simulation indicates [4, 5] that the uncertainty due to the beam energy will be bottleneck issue for improving the accuracy of τ mass measurement. Secondly, such kind of uncertainty is crucial for refining the determination of resonance parameters (say J/ψ

*Supported by the National Natural Science Foundation of China (10491303, 10775412, 10825524), the Instrument Developing Project of the Chinese Academy of Sciences (YZ200713), Major State Basic Research Development Program (2009CB825206), and Knowledge Innovation Project of The Chinese Academy of Sciences (KJCX2-YW-N29).

†E-mail:moxh@mail.ihep.ac.cn

and ψ') at BESIII. Last, small systematic uncertainty of the beam energy is also an indispensable factor for improving the measurement of branching ratio aiming at the accuracy of $1 \sim 2\%$.

Therefore, it is proposed to adopt the technique based on Compton backscattering principle to directly measure the beam energy with fairly high accuracy [6]. The detection system is determined to be allocated at the north interaction point (IP) of the BEPCII storage ring [7, 8] as shown in Fig. 1 and Fig. 2.

Unlike other systems where the High Purity Germanium (HPGe) detector is usually protected by radiation shielding wall [9, 10], the HPGe detector used at BEPCII has to be located near the vacuum tubes of the electron and positron beams in the storage ring tunnel. The irradiation field will definitely affect the proper performance of HPGe, one kind of high sensitive materials. Therefore, it is of paramount importance to measure the radiation dose at and/or around the position where the HPGe detector will be located.

Besides the safety considerations for HPGe, the radiological-safety protection for workers is another important factor for radiation dose measurement. According to Fig. 2, there is merely one shielding concrete wall with a thickness of 0.5 meter between the tunnel and the corridor for optics system, where some adjustment and inspection work should be performed. With all these in mind, it behooves us to know as much as possible the irradiation at the north IP. Therefore, the measurements of radiation dose are performed from February to March, 2008, and the results for γ, β, and neutron are obtained, according to which the shielding thickness for the safety of HPGe detector is estimated. Moreover, the photon background levels are measured in more details by NaI(Tl) detector, which provides useful information for the detector design and signal measurement in the future.

2 Measurement by Dosimeter

2.1 Two types of detectors

Two types of probes are used for radiation dose measurement and the first one is the optically stimulated luminescence detector (OSLD) made of carbon-doped aluminum oxide (Al_2O_3 :C) which is mainly used for γ, β and X-ray detection.

The optically stimulated luminescence (OSL) technique is now well-established for dosimetry applications on Earth (e.g. Lexel^{TM} dosimetry system, Landauer Inc. [11]) and its operational principle can be recapitulated as follows: (a) exposure of OSLD to ionizing radiation leads to the creation of electron/hole pairs via ionization and a fraction of the electrons and holes elevated to the conduction band by ionization then become trapped in defects within the structure of the OSL crystal; (b) subsequent thermal/optical stimulation releases these trapped charges leading to recombination of the electron-hole

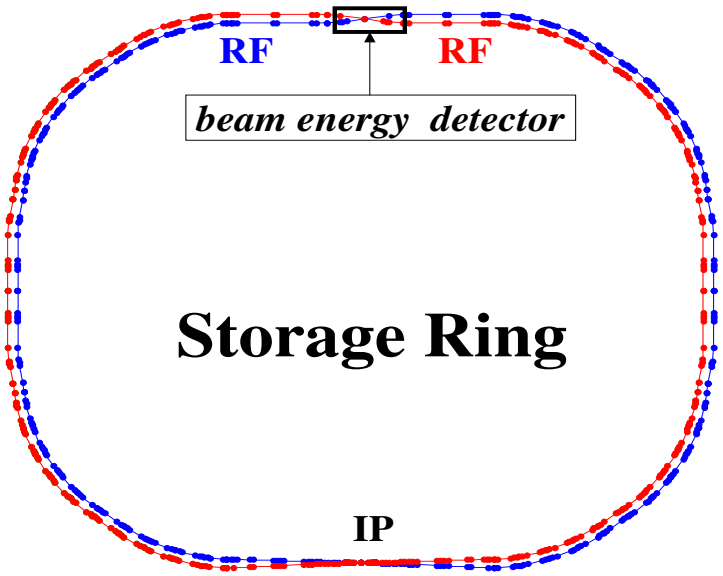

Figure 1: Schematic of the BEPCII storage ring. The interaction point (IP) located at the south cross point at the storage ring while the beam energy measurement system is allocated at the north.

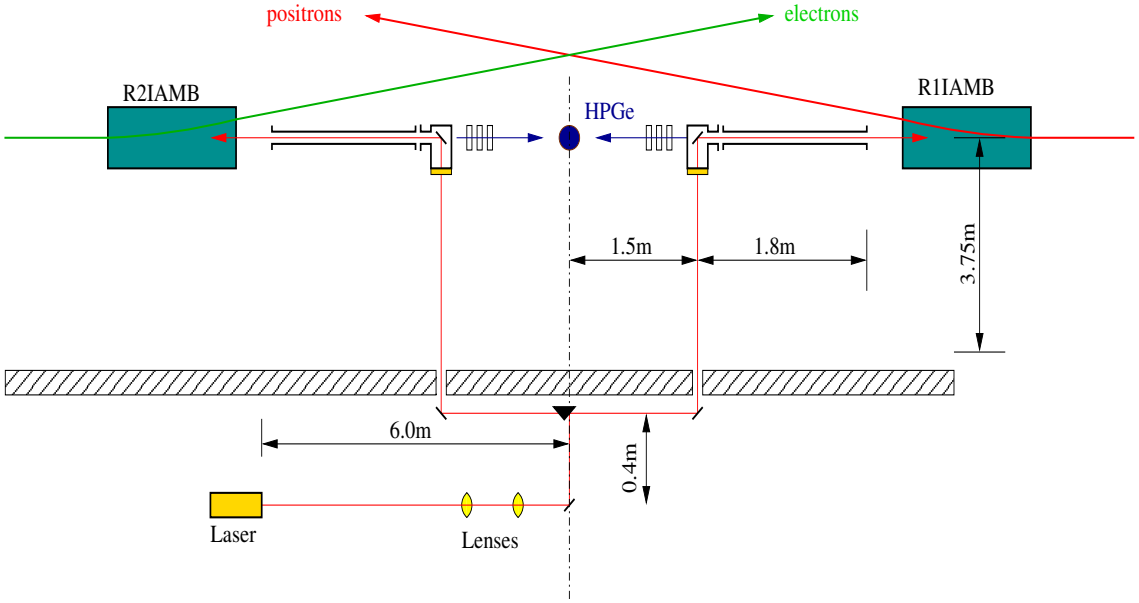

Figure 2: Simplified schematic of the beam energy measurement system. The positron and electron beams are indicated. R1IAMB and R2IAMB are accelerator magnets, and the HPGe detector is represented by the dot at the center. The half-meter shielding wall of the beam tunnel is shown cross-hatched. The laser and optics system will be located outside the tunnel.

pairs; (c) the recombination process results in light emission which can be detected and amplified by means of a photo-multiplier tube and related to the absorbed dose to which the dosimeter was exposed [12].

The readout of OSLD is realized by simply illuminating the dosimeter with light of appropriate wavelength and detecting the resulting light emission. The physics mechanism of OSL technique can be explained pedagogically by a simplest OSL model in which the OSL decay is given by [13]:

$$I_{\mathrm{OSL}}(\text{OSL decay intensity}) \approx n_0 f e^{-ft}, \tag{1}$$

where n_0 is the initial concentration of trapped charge carriers after irradiation, f is the wavelength-dependent optical excitation rate. This means that the rate of OSL decay and the level of the initial OSL intensity can be chosen by the appropriate stimulated intensity and wavelength. One can either have a high initial OSL intensity and fast decay (*i.e.* fast emptying of traps), or a low initial OSL intensity and slow decay (thereby probing just a fraction of the trapped charges).

The second type of detector is the solid state nuclear track detector (SSNTD) made of allyl diglycol carbonate[1]($C_{12}H_{18}O_7$), shortened as *CR*-39 which is mainly used for neutron detection.

SSNTDs are basically electrical insulating solid material in which the passage of heavily charged particles creates along their paths some damage zones on an atomic scale called **latent tracks**. The formation mechanism of these tracks is as follows [15]: when an ionizing particle interacts with matter, it transfers a part or the totality of its energy to the electrons of the medium with a linear rate of energy loss, dE/dx, which is a function of the particle characteristics (mass, charge, velocity) and of the detector material used[2]. When the energy loss is greater than a critical value (called *registration threshold* which is specific for the detector used), produced are local structure transformations which, in the case polymer such as *CR*-39, can be explained by ruptures in the molecular chains and/or formations of new components chemically very reactive along the particle trajectory. The latent track formed has a typical diameter from 1 to 10 nm [18]. With the help of

[1]The chemical structure of *CR*-39 can be expressed as $CH_2 = CH - CH_2 - O - CO - O - CH2CH2 - O - CH2CH2 - O - CO - O - CH2 - CH = CH2$. Its Chinese name can be found in Ref. [14]:

[2]The classical expression that describes the energy loss of particle within material is known as the *Bethe formula* and reads [16, 17]

$$-\frac{dE}{dx} = \frac{4\pi e^2 (ze)^2}{m_e v^2} \cdot NZ \cdot [ln\frac{2m_e v^2}{I} - ln(1 - \frac{v^2}{c^2}) - \frac{v^2}{c^2}], \tag{2}$$

where e and m_e are the electronic charge and the electron rest mass; *v(c)* and *ze* are the velocity (of light) and charge of primary particle; N and Z are the number of density and atomic number of the material atoms; I represents the average excitation and ionization potential of the material, and is normally treated as an experimentally determined parameter for special element.

chemical etching, the tiny latent track can be enlarged up to a diameter of few μm which is visualized under optical microscope. Then the work is track counting, and according to the relation between track parameters and particle energy loss information, the radiation dose will be determined eventually.

2.2 Landauer's service and measurement results

Figure 3: Landauer holder for OSLDs and SSNTDs with dimension 75 mm (length) $\times$ 36 mm (width) $\times$ 6 mm (thickness). The left is the synthetic one while the right shows the components which from the left to the right are CR-39 SSNTD, subcarrier, alligator clip, case with OSLDs, and plastic cover.

The radiation dosimeters used at BEPCII are provided by Landauer® incorporated company [11].

Landauer grows the special formulated $Al_2O_3 : C$ crystalline detector material which is then often configured into a laminated disk sandwiched within two mylars. So far as CR-39 is concerned, it is usually made into a small square. Used in this work is IZ-type dosimeter which actually consists of both I-type and Z-type dosimeters. The former is built on an assembly of a case component with metal and plastic filter along with a four-positioned OSLD slide component; while the latter is composed of one SSNTD and a ployethylene radiator; all components of IZ-type dosimeter are installed in the Landauer holder as shown in Fig.3. The standard holder has an alligator clip for secure fastening to clothing. Anyway in our experiment, the dosimeters are mainly used to measure the environmental dose, therefore holders are put on supports or fixed on the wall by adhesive tape.

Totally fifteen IZ-type dosimeters are used in two measurements, first time ten items and second five. The positions of each dosimeter are denoted in Fig. 4 and the detailed coordinates can be found in Table 1. The energies detected by OSLD ranges from 5 keV

Table 1: Results of radiation dose measurement. As indicated in Fig. 4, the "*O*"denotes the original of coordinate; the positive (negative) x-axis represents the east (west) direction; the positive (negative) y-axis represents the north (south) direction; $z = 0$ denotes the ground level of the storage ring tunnel and the positive (negative) z-axis represents the upwards (downwards) direction. The dosimeter at 8 is exposed in the air while the one at 8* is shielded by five-centimetre lead brick. The dose limits [17] for an occupational work is 100 mSv in 5 years and at the same time the dose can not be more than 50 mSv in any year.

serial number	Position (x, y, z) [cm]	Measured Dose $\gamma\&\beta$	Neutron [m Sv]
First measurment (3 days)			
①	(0,370,120)	6.44	0.07
② 2a	(300,0,10)	1.19	0.09
2b	(300,0,120)	1.36	0.12
2c	(300,0,270)	1.15	0.14
③ 3a	(−300,0,10)	0.58	0.12
3b	(−300,0,120)	0.74	0.07
3c	(−300,0,270)	0.67	0.07
④	(300,−50,110)	0.06	0.26
⑤	(−300,−50,110)	0.03	0.05
⑥	(−180,−240,30)	0.03	0.05
Second measurment (8 days)			
①	(0,370,120)	2.42	< 0.2
⑦ 7a	(0,0,10)	1.45	< 0.2
7b	(0,0,120)	2.47	< 0.2
⑧ 8	(−250,300,100)	1.20	< 0.2
8*	(−250,300,90)	< 0.01	< 0.2

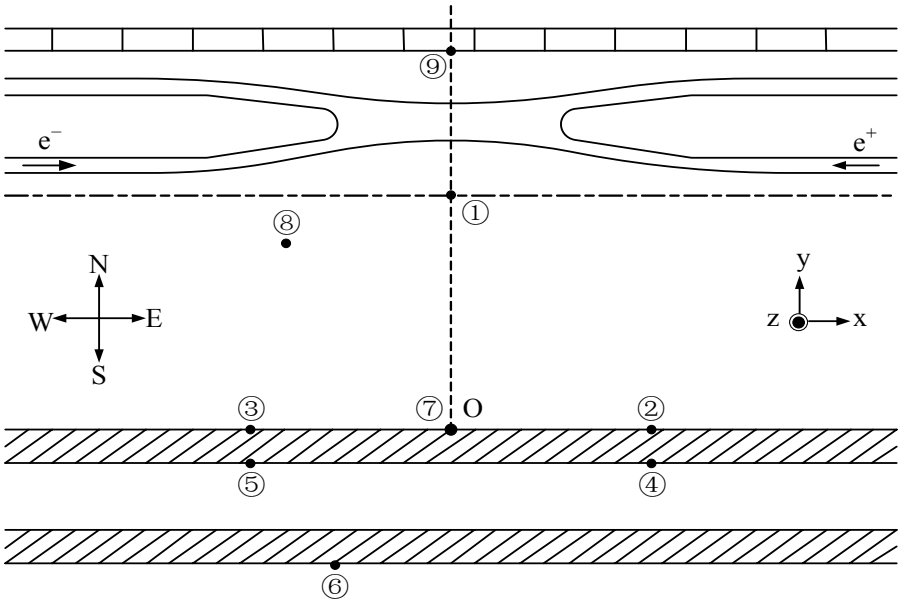

Figure 4: Vertical view of the BEPCII north interaction point(IP). The "O" denotes the original of coordinate which does not coincide with the north IP. Two hatched bands indicate the two concrete walls with thickness 50 cm each; the top block band denotes the support for various wires and cables; and the two bands crossed at IP delineate the vacuum pipes for the electron and positron beams. The circled numbers indicate the dosimeter sites.

to 40 MeV for γ and X-ray; and from 150 keV to 10 MeV for β particle while the energies detected by SSNTD range from 40 keV to 40 MeV for fast neutron. The corresponding doses measured are from 0.01 mSv to 10 Sv (γ and X-ray), 0.1 mSv to 10 Sv (β), and 0.2 mSv to 250 mSv (neutron), respectively. It should be noted here that the conditions for measurements at two different times are rather distinctive. For the first measurement, both positron and electron beams are with intensity around $400 \sim 500$ mA, and duration is about 3 days. For the second time, only electron beam exists, with intensity around $200 \sim 250$ mA, and duration is about 8 days.

When the measurement is finished, all dosimeters are collected and returned to Landauer for analysis. The $Al_2O_3 : C$ detector is read out by OSL technique. The reader stimulates the detector with a light emitting diode array causing it to luminesce in proportion to the amount of radiation exposure. The luminescence is detected and measured by the reader's photo multiplier tube using a high sensitivity photon counting system. A dose calculation algorithm is then applied to the measurement to determine exposure results. For neutron analysis, the CR-39 is etched for 15 hours in a chemical bath to enlarge exposure tracks. The fast neutron dose is measured by counting the tracks generated as a result of the proton recoil with the polyetheylene radiator. After one or two months,

all measurement results tabulated in Table 1, are back from Landauer company to IHEP by registration post.

2.3 Discussion

By virtue of the information provided in Fig. 4 and Table 1, general understanding of radiation at the north IP is obtained. Let us begin with the first time measurement for γ and β.

Firstly, the radiation dose at ① is 6.44 mSv which is about 200 times higher than that at ⑥, 0.03 mSv which is safe for human activity. If the same level of low radiation as point ⑥ is required around point ① where HPGe will be located, some shielding materials are needed. As a simplistic and conservative estimation, the needed thickness of lead is calculated by the following formula

$$D_x = D_0 e^{-\mu x}, \text{ or } x = \frac{1}{\mu} \cdot \ln \frac{D_0}{D_x}, \tag{3}$$

where μ is the linear attenuation coefficient in shield material for the photons of the energy concerned; x is the shield thickness; D_0 is the unshielded dose while D_x the shielded dose at a point of interest behind the shield. Values of μ are available in a variety of sources [19] and a few of them relevant to the analysis are listed in Table 3. Specially for our case, for $E_\gamma \approx 8$ MeV, with $D_0/D_x \approx 200$ and μ =0.55, it yields $x \approx 9.63$ cm by virtue of Eq. (3). More meticulous calculation indicates $x \approx 11.37$ cm which is compatible with the simplified estimation[3].

Secondly, if comparing the measurements of a, b, and c at the positions of ② or ③, it can be seen that the radiation dose at b is greater than those at a and/or c which means the radiation at the plane of the vacuum pipe is greater than at the other horizontal planes.

Thirdly, as shown in Fig. 4, on the east (west) side of IP, the positron (electron) beams run in the inner-ring which are close to the wall. Since the radiation due to positron is greater than that of electron, the radiation dose around positron ring is expected greater than that of electron. This is confirmed from our measurement. When comparing two sets of measurements at the positions of ② and ③, it is obvious that radiation doses at ② are almost two times greater than those at ③.

So far as the neutron background is concerned, the results listed in Table 1 indicate that radiation dose at ① (0.07 mSv) is almost the same as that at ⑥ (0.05), therefore, the effect of neutron radiation on HPGe is fairly small. However, the neutron dose at ④ is 0.26 mSv, and at 2*b* is 0.12 mSv, this is contradictory to the expectation that the dose

[3]Refer to the appendix of this paper for more detailed evaluation.

at $2b$ should be larger than that at ④. Therefore further measurements need to clear up the issue.

Qualitatively, the results of the second measurement are reasonable as well. It should be noted here, since the conditions differ considerably for two measurements, and the irradiation fields distribute rather complicatedly, it is hard to compare two kinds of measurements in a simple way. Last but not the least, the measurement results at 8 and 8* indicate that the lead shielding can greatly decrease the radiation dose of γ and β. This measurement also qualitatively consists with the estimation obtained by Eq. (3).

3 Measurement of the γ-spectra with NaI(Tl) detector

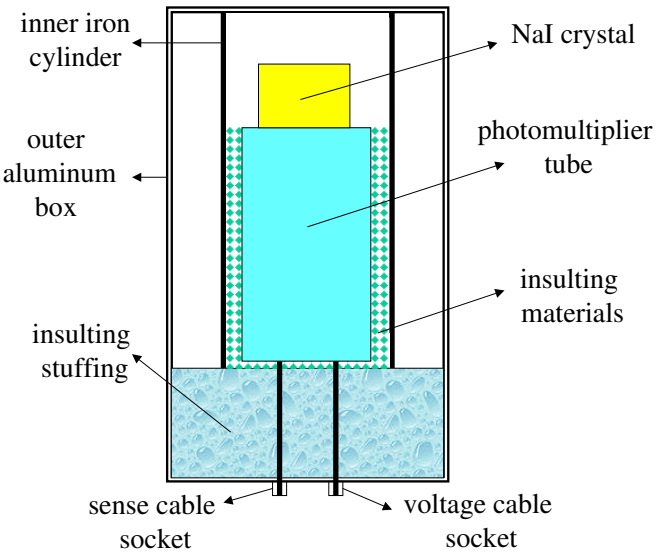

Figure 5: Sketch of NaI(Tl) detector. NaI(Tl) crystal (ϕ45 mm × 40 mm) coupled on photomultiplier GDB50, put in a magnetic shielding cylinder (ϕ 7 cm × 23.6 cm with a thickness of 2 mm) made of soft iron, and encapsulated in an aluminum box (10 cm × 10 cm × 32 cm with a thickness of 2 mm).

HPGe detector is an expensive instrument, and such a detector has never been located at the interaction point of BEPCII for the measurement of γ-/X-rays energy spectra. In order to acquire the practical conditions for HPGe, a NaI(Tl) detector (refer to Fig. 5 for its construction) is used, which is similar to an ordinary HPGe detector in detection efficiency of γ-rays. This γ-spectrometer system was consisted of the NaI(Tl) crystal (ϕ45 mm × 40 mm), photomultiplier GDB50, and 8192 MCA, of which, the energy resolution

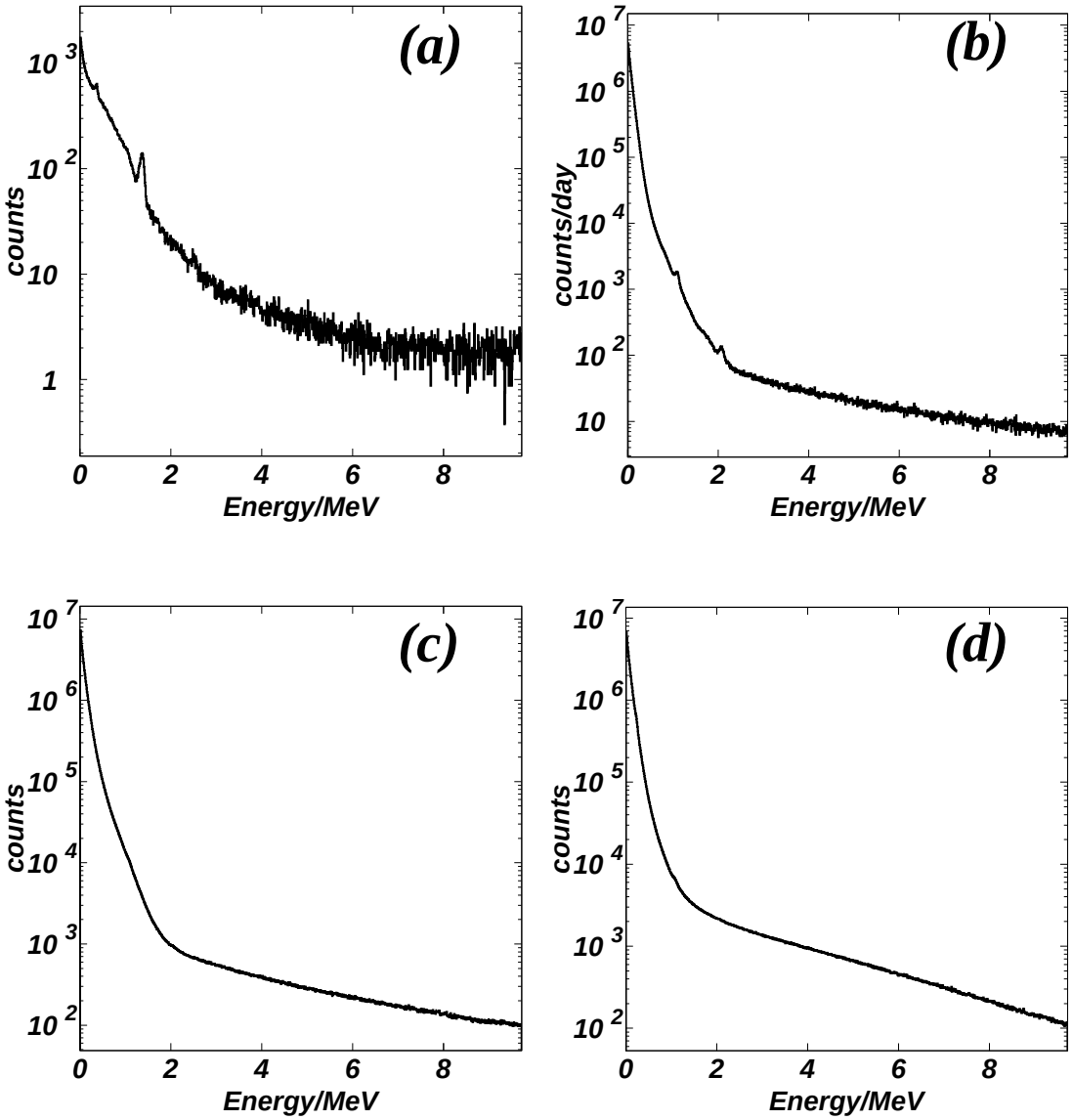

Figure 6: Data recorded by NaI(Tl) detector at the north IP for case (a), (b), (c), and (d) as described in the text. Two peaks in (a) appear at 0.35∼0.36 and 1.34∼1.35 MeV, and in (b) at 1.07∼1.08 and 2.02∼2.03 MeV, respectively.

is FWHM=9.5% for ^{137}Cs 662 keV γ-ray and the peak/valley $\approx$ 3:1 for ^{60}Co 1.33 MeV γ-ray, respectively. With the γ-spectrometer, four measurements denoted as case (a), (b), (c), and (d) are performed respectively at three points. The distributions of these points can be referred to Fig. 4 while the special coordinates of them are presented in Table 2. First two measurements, cases of (a) and (b), are carried out at the same position, that is point ⑧. For case (a), the NaI(Tl) detector is encapsulated by lead bricks with a thickness of 5 cm while for case (b), there is no radiation shielding of this kind. The measurements of cases of (b), (c), and (d), are performed at the points of ⑧, ①, and ⑨, respectively, all without lead-brick shielding. These results can be compared to understand the radiation distribution in the region of the north IP.

Some results[4] are exemplified in Fig. 6 and Table 2. The interesting information concerned includes: the total counts (N_{tot}) for each case; the counts between energies 2 MeV and 7 MeV (N_{2-7}) which correspond to the designed beam energies (E_{beam}) of BEPCII ranging from 1 GeV to 2 GeV; in addition, the counts at energy 5.64 MeV ($N_{5.64}$) which corresponds to the τ mass energy (E_{beam}=1.777 GeV).

Next we analyze the information and data in Fig. 6 and Table 2. Firstly, for plots (b), (c), and (d) of Fig. 6, a high counting rate ($\sim 10^4$ cps) concentrates ($\sim$ 90%) below 200 keV, which can be attributed to the bremsstrahlung emissions from high velocity electrons and the multi-Compton scattering processes from high energy photons. It should be noted that a very high counting rate appears at low energy region (with energy below 20 keV), which must be prevented in the future measurements with HPGe because it may affect the measured precision due to the pile-up effect in electronics. Fortunately, the background in the lower energy region has been strongly suppressed by using a lead shielding, see plot Fig. 6(a) and refer to the numbers for case (a) in Table 2.

Secondly, the backgrounds, especially in Fig. 6(a), are quite low at the energies higher than 2 MeV (the corresponding proportion of counts is less than 1%), which is beneficial for future beam measurements.

Thirdly, two weak peaks appear in plots of (a) and (b), which should be investigated carefully in the future with our HPGe (a high resolution spectrometer), if necessary.

Last, the photon background with energy between 2 MeV and 7 MeV is less than 1% (N_{2-7}/N_{tot}) for cases of (b), (c), and (d). For the photon background with energy at 5.64 MeV, the number of largest counts only amounts to 6×10^{-7} per second which is small enough to be neglected [6].

[4]The experiment begins on February 19th, 2008 and ends on March 17th, 2008, with totally 28 days. The measurement results are recorded automatically in a series of files and the interval for each file is three hours. All files are surveyed and a few of them are selected which reflect the comparatively stable running state of BEPCII.

Table 2: Measurement results of NaI(Tl) detector corresponding to the cases of (a), (b), (c), and (d) in Fig. 6. Besides the experiment dates, integrated current, and detector positions, the following information is provided: the total counts (N_{tot}) for each case; the counts between energies 2 MeV and 7 MeV (N_{2-7}); the counts with energy below 2 MeV ($N_{<2}$); the counts at energy 5.64 MeV ($N_{5.64}$). Besides the numbers of counts per day, the numbers of counts per second (sec.) are also listed for N_{tot} and N_{2-7}.

	Case (a)	Case (b)	Case (c)	Case (d)
date/yy.mm.dd	2008.2.22	2008.2.29	2008.3.8	2008.3.17
position/cm	⑧ (−250,300,115)		① (0,370,115)	⑨ (0,615,135)
Int.Curr./A·H	4.45	4.42	4.58	4.99
N_{tot}/day	5.00×10^5	3.23×10^8	5.75×10^8	5.28×10^8
N_{tot}/sec.	5.79	3.73×10^3	6.66×10^3	6.11×10^3
N_{2-7}/day	2.26×10^4	1.24×10^5	1.58×10^6	3.74×10^6
N_{2-7}/sec.	0.26	1.44	18.34	43.28
$N_{<2}$/day	4.31×10^5	3.22×10^8	5.71×10^8	5.23×10^8
$N_{5.64}$/day	3	16	228	497

4 Summary

Understanding the irradiation around the north IP is the main purpose of the measurement work depicted in this monograph. To this end, the backgrounds due to γ, β, and neutron radiation are firstly measured by IZ-type dosimeters provided by Landauer Incorporated Company. The analyzing of measurement results indicates that the will-be HPGe detector with practical protection can work stably and durably without damage at the north IP of BEPCII.

In order to figure out the photon background in more detail, a special NaI(Tl) detector is constructed and utilized to acquire the irradiation information in the vicinity of the north IP. The experiment results indicate that the photon contamination as background for further measurement is small enough and can be handled readily.

However, further studies are necessary due to many factors. Firstly, because at the beginning of accelerator commission, our measurements are performed under a rather different condition from that of real running. Therefore, more experiments are needed to proceed under the condition more similar to the actual running. Secondly, more experimental points are needed to obtain comparatively accurate distributions of radiation. Thirdly, the detection accuracy of neutron should be improved to clear up the puzzle observed. Last, more information can enhance the reliability of estimation for radiological-safety protection.

Appendix: Calculation of shielding thickness

All data compiled in this appendix and more information about radiation protection are available in many references[5]. Herein the evaluation of shielding thickness is based on the measurement results provided in Table 1.

Table 3: Shielding thickness (in unity of cm) for multiple of attenuation k and the linear attenuation coefficients for photon μ.

E_γ (MeV)	Multiple of attenuation k				μ (cm^{-1})
	10^2	2×10^2	5×10^2	10^3	
Concrete (density $\rho = 2.3$ g/cm^3)					
1	50.5	56.4	64.6	70.4	0.141
2	65.7	74.0	84.5	92.7	0.100
3	77.5	88.0	101.0	110.9	0.080
4	84.5	95.7	110.4	120.9	0.071
6	95.1	108.0	124.4	137.9	0.061
8	98.0	112.1	129.7	143.2	0.058
10	105.1	120.9	139.7	155.0	0.053
Lead (density $\rho = 11.34$ g/cm^3)					
1	7.0	8.0	9.2	10.2	0.79
2	11.3	12.9	15.0	16.5	0.51
3	12.2	14.0	16.3	18.0	0.46
4	12.1	13.8	16.1	17.8	0.47
6	10.9	12.6	14.9	16.5	0.51
8	9.9	11.4	13.3	15.1	0.55
10	8.7	10.2	11.9	13.3	0.60

Many tables are available to estimate the shielding thickness of various materials under certain photon energy. Taking the measurement expounded in the paper as a special example, the energy of radiation photon (γ) can be derived from Table 3. Firstly, in the light of data in Table 1 , the attenuation between point ① and ⑥ equals to 200 (that is $k = 2\times10^2$ in Table 3). Secondly, the summed thickness of two walls (which are made by concrete and treated as shielded materials) is around 100 cm (refer to Figure 4), then the corresponding photon energy (E_γ) can be found in Table 3. Notice that E_γ could be in the range from 6 MeV to 10 MeV according to the information of Table 3. As a rough estimation, $E_\gamma \approx 8$ MeV is taken, together with $k = 2\times10^2$, then utilizing Table 3 again,

[5]For example, *Manual of Radioisotope*, compiled by Ma C Z *et al.*, Beijing, Science Press (1979)

Table 4: The dose buildup factor B which represents the ratio of the total dose to the primary photon dose (the primary photon dose comes from original photons that have penetrated the shielding material without interacting) and depends on γ source and shield characteristics.

E_γ (MeV)	μ				
	1	2	4	7	10
Concrete					
1	1.94	3.10	5.98	11.65	18.70
2	1.75	2.52	4.38	7.65	11.40
3	1.60	2.24	3.64	5.99	8.58
4	1.49	2.01	3.12	4.96	6.99
6	1.38	1.79	2.64	4.10	5.76
8	1.31	1.62	2.30	3.47	4.82
10	1.24	1.48	2.03	3.00	4.15
Lead					
1	1.37	1.69	2.26	3.02	3.47
2	1.39	1.76	2.51	3.66	4.84
3	1.34	1.68	2.43	2.75	5.30
4	1.27	1.56	2.25	3.61	5.44
6	1.18	1.40	1.97	3.34	5.69
8	1.14	1.30	1.74	2.89	5.07
10	1.11	1.23	1.58	2.52	4.34

the shielding thickness for lead is obtained to be 11.4 cm which is compatible with the estimation by Eq. (3).

When the energy of radiation source is well known, the theoretical calculation is more favorable, such as the aforementioned evaluation in Section 2.3. However, some actual effects, such as material scattering and secondary radiation, have not been taken into consideration in previous evaluation. The added effect of various actual reactions is usually taken into account by incorporating a so-called buildup factor B into Eq. (3), that is

$$D_x = D_0 \cdot B(x, E_\gamma) \cdot e^{-\mu x} \tag{A. 1}$$

where the meaning of D_0, D_x, μ and x are the same as those in Eq. (3). Here the magnitude of B depends on the shielding thickness x, photon energy (E_γ), also on the special geometry of experiment. Notice the dependence of B on x, the more reliable estimation of x value can be acquired by successive approximation approach with the help of existing information for B, such as the data tabulated in Table 4. The special

steps are listed as follows:

1. Roughly estimating a value of μx (for example using the value from Eq. (3), then finding the corresponding buildup factor B from Table 4 (the value between those listed in Table 4 can be obtained by interpolation)).

2. Substituting the value B in Eq. (A. 1) and finding μx.

3. By virtue of this calculated μx, finding the factor B again from Table 4.

4. Replacing this B value in Eq. (A. 1), the value μx can be obtained.

The value μx acquired through four steps above is used to computer x. From the last column of Table 3, the μ value for certain E_γ can be read and then the value x can be calculated accordingly. More repetition of Step 3 and 4 can lead to more accurate estimation of x. Under our cases, one iteration yields x=11.33 cm and two iterations yield x = 11.37 cm which consists fairly well with the value presented in Table 3.

References

[1] *Physics at BESIII* [arXiv.0809.1869], Eds. Kuang-Ta Chao and Yifang Wang (September, 2008)

[2] YUAN Chang-Zheng, ZHANG Bin-Yun, QIN Qing. HEP & NP **26**, (2004) 1201-1208 (in Chinese)

[3] FU Cheng-Dong, MO Xiao-Hu. Chin. Phys. C 2008, **32**: 776-780

[4] Mo X H. Nucl. Phys. B (Proc. Suppl.) 2007, **169**: 132-139

[5] Wang Y K, Mo X H, Yuan C Z, Liu J P. Nucl. Instr. Methd. 2007, **A583**: 479-484

[6] MO Xiao-Hu *et al.* Chin. Phys. C 2008, **32**: 995-1002

[7] *Design Report of accelerator BEPCII (Accelerator Part)* (May, 2002); also could be obtained through web page:
http://acc-center.ihep.ac.cn/download/pdr_download.htm

[8] Achasov M N *et al.* "*The beam energy calibration system for BEPCII collider*", arXiv:0804.0159 [physics.acc-ph]

[9] Hsu I C, Chu C-C, and Yu C-I. Phys. Rev. E54 (1996) 5657

[10] Ohgaki H *et al.* Nucl. Instr. Methd. 2000, **A455**: 54-59

[11] The detailed and comprehensive introduction about Inlight dosimeters could be found through web page:
http://www.landauerinc.com/

[12] Yukihara E G *et al.* Radiation Meaurement **41** (2006) 1126-1135

[13] McKeever S W S. Nucl. Instr. Methods **B 184** (2001) 29-54

[14] Zhuo W H *et al.* Atomic Energy Science and Technology suppl. **42** (2008) 322-325

[15] Amgaron K. "*Long-term measurements of Indoor Radon and its progeny in the presence of Thoron using nuclear track detectors: a novel approach*", Ph.D. thesis (April, 2002)

[16] Knoll G G. "*Radiation detector and measurement*", Juhn Wiley & Sons (1979)

[17] Leo W R "*Techniques for nuclear and particle physics experiments*", Springer-Verlag, Berlin (1994)

[18] Fleischer R L, Price P B, Walker R M. "*Nuclear tracks in solids: principles and applications*", University of California Press, Berkely (1975)

[19] Values of μ are available at NIST (National Institute of Standards and Technology) web site:
http://physics.nist.gov/PhysRefData/XrayMassCoef/cover.html